Temperature-Dependent Anti-Stokes/Stokes Ratios under Surface-Enhanced Raman Scattering Conditions

R. C. Maher,*,† L. F. Cohen, and J. C. Gallop

The Blackett Laboratory, Imperial College London, Prince Consort Road, London SW7 2BW, United Kingdom

E. C. Le Ru and P. G. Etchegoin‡

The MacDiarmid Institute for Advanced Materials and Nanotechnology, School of Chemical and Physical Sciences, Victoria University of Wellington, P.O. Box 600, Wellington, New Zealand

Received: November 8, 2005; In Final Form: January 5, 2006

We make systematic measurements of Raman anti-Stokes/Stokes (aS/S) ratios using two different laser excitations (514 and 633 nm) of rhodamine 6G (RH6G) on dried Ag colloids over a wide range of temperatures (100 to 350 K). We show that a temperature scan allows the separation of the contributions to the aS/S ratios from *resonance effects* and *heating*/*pumping*, thus decoupling the two main aspects of the problem. The temperature rise is found to be larger when employing the 633 nm laser. In addition, we find evidence for mode specific vibrational pumping at higher laser power densities. We analyze our results in the framework of ongoing discussion on laser heating/pumping under surface-enhanced Raman scattering (SERS) conditions.

I. Introduction

Despite rapid progress on Surface Enhanced Raman Scattering (SERS)[1,2] toward applications,[3−6] many fundamental questions remain open. An important issue that has been the subject of controversy relates to whether the local enhanced electromagnetic (EM) fields cause local heating and/or vibrational pumping. This is important for reasons that range from the purely practical (damage to analytes under study) to the more fundamental (vibrational pumping). In certain cases, plasmon-related heating effects may even be useful[7] for biomedical applications, but both the magnitude of the effect and how to control it need proper characterization. It is possible to use the anti-Stokes/Stokes (aS/S) ratio under SERS conditions to study heating/pumping effects with certain limitations, as we discuss in detail below.

The laser power dependence of the aS/S ratio was thought to provide strong evidence for SERS pumping,[8] but this has been the source of controversy and alternative explanations have been offered.[9−12] Contributions to the aS/S ratio can be complex and include heating, pumping, and resonance effects. There are various hints for heating in SERS and the anomalous ratio (commonly measured even at low powers) was predicted to relate to hidden resonances in the system.[10,11] We have recently demonstrated that it is indeed possible to use the aS/S ratio to map out roughly the underlying resonance in certain cases.[13]

Here we develop the use of aS/S ratios further; we expand and provide additional evidence to recent discussions in refs 12 and 14. We demonstrate how to separate heating from resonance effects through temperature (*T*)-dependent data. We find a temperature rise at low laser powers (≈0.5 mW on a ∼1.5 μm (diameter) spot) that depends on laser energy. We find evidence also suggesting the existence of mode specific vibrational pumping at higher laser power densities and low temperatures.

II. General Considerations

For the sake of clarity we shall repeat the essential details of the discussion presented in refs 12 and 14, keeping details to a minimum. We call T_{env} the temperature of the local environment (substrate + ambient surrounding the sample), while T_{room} is room temperature, T_{met} the temperature of the metal colloids, and T_{mol} the temperature of the molecule. The main possible scenarios are the following:

1. No heating: The whole system is in thermal equilibrium, i.e., $T_{room} = T_{env} = T_{met} = T_{mol}$.

2. Global heating: The system is in thermal equilibrium at a T higher than T_{room}, i.e., $T_{env} = T_{met} = T_{mol} > T_{room}$.

3. Local heating of the substrate and the analyte: $T_{mol} = T_{met} \geq T_{env} \geq T_{room}$. The analyte is in thermal equilibrium with the metal, at a higher temperature than their environment. The source of heating here is mainly laser absorption in the metal substrate.

4. Local heating of the analyte: $T_{mol} \geq T_{met} \geq T_{env} \geq T_{room}$. Here the molecule remains in internal thermal equilibrium at a temperature T_{mol}, higher than the rest of the system. Strong interactions among vibrational modes within the molecule allow vibrational energy to thermalize and reach an equilibrium through intramolecular vibrational relaxation or redistribution (IVR). The source of heating here can be direct laser absorption in the molecule (via electronic state transitions) or vibrational pumping (via SERS processes) followed by fast IVR. However, it is difficult to distinguish between these two possible causes.

5. Mode specific vibrational pumping: The analyte is not in internal thermal equilibrium. Each vibrational mode can be described by an effective mode temperature, T_i^{eff}, that reflects the population of its first vibrational excited state.[12] In general, IVR ensures that T_i^{eff} is the same for all modes (internal thermal equilibrium at a temperature T_{mol}). However, SERS

* Address correspondence to this author.
† E-mail: robert.maher@imperial.ac.uk.
‡ E-mail: pablo.etchegoin@vuw.ac.nz.

10.1021/jp056466r CCC: $33.50
Published on Web 03/11/2006

processes affect the vibrational population and can pump vibrations from the ground to the first excited vibrational state (for Stokes processes). If for a given vibrational mode the pumping rate becomes comparable or higher than the IVR rate, this mode can then have a higher effective temperature than the other modes: $T_i^{\text{eff}} \geq T_{\text{mol}} \geq T_{\text{met}} \geq T_{\text{env}} \geq T_{\text{room}}$; this is referred to as *mode specific pumping*.

The different scenarios deserve a brief comment. If vibrational pumping occurs in the presence of fast IVR, pumping will only be observed as an effective heating of the molecule (4th scenario). From the experimental point of view, under these circumstances, it would be impossible to distinguish this situation from the 3rd scenario. It is indeed very difficult to determine independently the temperature of the metal and the molecule, due to the lack of a spectroscopic feature coming explicitly from the metal. Even if one could prove that the 4th scenario was the correct one, it would then be extremely difficult to determine the real cause of heating: direct laser absorption or vibrational pumping, or a combination of both effects. Consequently, the only clear-cut demonstration of vibrational pumping is, in our view, the last scenario, i.e., mode specific pumping. Heating and pumping under SERS conditions have previously been investigated with use of peak parameter correlations, such as width or frequency vs intensity.[12,15] Evidence was found for local heating (3rd or 4th scenario) but no evidence of mode specific pumping was uncovered.[12] Although yielding evidence for the existence of local heating, it was impossible to distinguish its origin, i.e., either within the molecule itself or the colloid (and consequently the molecule through its close contact with the metal). These previous results do not exclude the presence of pumping (vide supra) but they do not demonstrate it either.

Most other studies of heating/pumping under SERS conditions[8−11] have focused on the measurements of the aS/S ratio, ρ. This ratio is in principle directly related to the vibrational populations, and therefore to the effective mode temperature. However, in the case of SERS, it can be modified by underlying resonances associated with the wavelength dependence of the SERS enhancement factor, making the interpretations more difficult. The most general expression for the ratio under SERS conditions at low powers (in the absence of pumping) and for molecules in thermal equilibrium at a temperature T_{mol} is[16,17]

$$\rho = \frac{I_{\text{AS}}}{I_{\text{S}}} = A_\omega \frac{\sigma_{\text{AS}}}{\sigma_{\text{S}}} \sum_{j=1}^{N} \frac{A_{\text{AS}}^j}{A_{\text{S}}^j} \exp(-\hbar\omega_{\text{v}}/k_{\text{B}}T_{\text{mol}}) \qquad (1)$$

with $A_\omega = (\omega_{\text{L}} + \omega_{\text{v}})^4/(\omega_{\text{L}} - \omega_{\text{v}})^4$ (accounting for the standard wavelength dependence of Raman processes). $I_{\text{AS(S)}}$ is the intensity of the anti-Stokes (Stokes) Raman mode, $\omega_{\text{L(v)}}$ is the frequency of the laser (Raman mode), $\sigma_{\text{AS(S)}}$ is the anti-Stokes (Stokes) scattering cross section of the molecule, N is the number of active molecules, and $A_{\text{AS(S)}}$ is the SERS enhancement factor at the molecule position at the anti-Stokes (Stokes) frequency. The latter term includes both electromagnetic and chemical enhancement effects. In general the enhancement can be site dependent and therefore should be summed over all active sites. Because anti-Stokes signals are typically small, their measurement requires relatively long integration times and/or large analyte concentrations. The results are therefore an average over several active sites/molecules, each with different enhancement factors and resonances. To account for this averaging, ρ for a given mode i can be modeled in a first approximation as

$$\rho_i = A_\omega A_i \exp(-\hbar\omega_i/k_{\text{B}}T_i^{\text{eff}}) \qquad (2)$$

where A_{i} is the average *asymmetry factor* from resonance effects (asymmetries in cross sections), which can change from mode to mode. T_i^{eff} was used in this expression to account for the possibility of different effective mode temperatures. When the vibrational pumping rate is small compared to the IVR rate, we have $T_i^{\text{eff}} = T_{\text{mol}}$ for all modes and the molecule is in thermal equilibrium at T_{mol}. However, if vibrational pumping is not negligible, this expression needs to be modified to give (for weak pumping)[8,10,12]

$$\rho_i = A_\omega A_i[\exp(-\hbar\omega_i/k_{\text{B}}T_{\text{mol}}) + \sigma_{\text{S}}\tau_{\text{r}}I_{\text{L}}] \qquad (3)$$

where τ_{r} is the vibrational relaxation time (including IVR and other relaxation processes), and I_{L} is the laser intensity in photons per unit time and surface area. We see in this latest expression that vibrational pumping would tend to increase the value of ρ_{i}. This could alternatively be described by eq 2, using an effective mode temperature $T_i^{\text{eff}} > T_{\text{mol}}$, but determining T_i^{eff} would require the use of eq 3.

Equation 2 or 3 forms the basis for the analysis of most SERS experiments about heating/pumping that use aS/S ratio measurements. From them, it is obvious that the measurement of ρ_i only is not sufficient to extract T_{mol} or T_i^{eff}, as the A_i values are unknown. One therefore needs an extra free parameter. In previous works, the power dependence of ρ_i, for example, was studied.[8,10,15] A linear dependence of ρ_i with I_{L} has been invoked as evidence of vibrational pumping that would appear to follow from eq 3. This is not true, however, and direct heating of the molecule has been proposed as an alternative explanation.[11] Equations 2 and 3 form the basis to understand the effect of heating on ρ, one can write $T_{\text{mol}} = T_0 + \Delta T$, and expand eq 2 considering a small temperature increase, $\Delta T \ll T_0$:

$$\rho_i = A_\omega A_i \exp\left(-\frac{\hbar\omega_i}{k_{\text{B}}T_0}\right) \exp\left(\frac{\hbar\omega_i}{k_{\text{B}}T_0}\frac{\Delta T}{T_0}\right) \qquad (4)$$

If heating effects are present, ΔT changes with power. Because heat diffusion and transfer models are linear, it is reasonable to assume that the temperature increase ΔT is proportional to laser power: $\Delta T = aI_{\text{L}}$. For a small temperature increase, the argument in the second exponential of eq 4 is small and expanding it leads to

$$\rho_i = A_\omega A_i \exp\left(-\frac{\hbar\omega_i}{k_{\text{B}}T_0}\right)\left(1 + \frac{\hbar\omega_i}{k_{\text{B}}T_0}\frac{a}{T_0}I_{\text{L}}\right) \qquad (5)$$

The linear dependence of ρ_i (or quadratic dependence of I_{AS}) with incident power can therefore equally be the result of conventional heating effects or of pumping. It is also worth noting that the argument in the second exponential of eq 4 can be comparable to 1, even for a small ΔT. This can be the case for example for high energy modes, where $\hbar\omega_i/k_{\text{B}}T_0$ can be $\approx$10. The power dependence of ρ_i as a result of heating effects would then be exponential. Such power dependence, linear for low-energy modes and exponential for high-energy modes, has already been observed.[15] This shows that heating effects can be important and that a linear power dependence of ρ_i is not in itself a proof of vibrational pumping.

Instead of using the laser power as an additional parameter, we propose to study the aS/S ratios of each mode as a function of substrate temperature T_0. As we shall show, by investigating how these ratios change as a function of T over a wide range,

we can separate the contributions due to heating and resonance effects. In addition, this approach enables us to detect a departure from internal thermal equilibrium of the molecule, i.e., vibrational pumping.

III. Experimental Details

Silver colloids were produced as described in ref 18. SERS samples were prepared by mixing equal amounts of colloidal and 25 mM KCl solutions together, to which 1 μL of 10^{-6} M Rhodamine 6G (RH6G) solution was added, resulting in a 10^{-9} M RH6G concentration. The sample was then dried onto a Si substrate. The temperature calibration in terms of aS/S data of non-SERS active signals (paracetamol) is described elsewhere.[14] Measurements were carried out with a Renishaw 2000 CCD spectrometer and an Olympus BH-2 microscope with a Linkham temperature stage, using both 514 nm Ar^+ ion and 633 nm HeNe lasers with a $\times 50$ long working distance objective ($\sim$1.5 μm beam diameter at the focal point). Measurements with the 514 nm laser were made at 0.5 mW, whereas for the 633 nm laser they were performed at 0.5 and 5 mW, respectively, in the range between 100 and 350 K in steps of 10 K and integration times varying from 1 to 30 s. Five or more measurements were made to gain an average over the sample. Peaks were then analyzed by using standard Voigt functions with subtracted backgrounds.

The variation in the aS/S ratio for each mode was fitted to eq 2, with $T_i^{\text{eff}} = T_{\text{Si}} + \Delta T_i$, where ΔT_i is the increase in effective mode temperature with respect to the T of the substrate, which is measured by the aS/S ratio of the Si substrate.[14] The parameters A_i in eq 2 will depend on the particular mode under consideration, accounting for the asymmetry in σ_S and σ_{AS} produced by resonances. Four types of fits were performed: ΔT-only, where A_i is set to 1 (no resonance effect) and ΔT_i are fitting parameters; A-only, where $\Delta T_i = 0$ (no local heating, no pumping) and A_i are fitting parameters; $A + \Delta T$-shared, where $\Delta T_i = \Delta T$ is constant for all modes and A_i are fitting parameters (this corresponds to the case of internal thermal equilibrium for the molecule); and $A + \Delta T$, where A_i and ΔT_i are independent fitting parameters (this allows the modes to have different effective mode temperatures).

Figure 1 illustrates the predictions of the model and the influence of A and ΔT on the value of the aS/S -ratio as a function of T. Figure 1a shows the expected value of the ratio for different A values, while keeping $\Delta T = 0$. When $A < 1$ ($A > 1$) the ratio is suppressed (increased). In Figure 1b A is held constant while ΔT is varied: the influence of ΔT is strongest at low T values where it is a greater fraction of the initial T, resulting in a distinctive "flaring" of the ratio at low T values and a flattening of the overall curve shape.

The first two types of fits are only used to test whether a simple model with heating only and no resonances, or resonances only and no heating, is sufficient to explain the data. For all fits, we assume that A_i and ΔT_i are constant with temperature. A_i, which is the result of predominantly electromagnetic resonances, is not believed to vary with temperature. For molecules in thermal equilibrium $\Delta T_i = \Delta T$ is the same for all modes and represents the temperature increase (heating). Many factors contribute to this increase, for example, the thermal properties of the SERS substrate and of the various interfaces. These factors could possibly vary with temperature, although large variations typically occur mainly at even lower temperatures ($T < 100$ K). The assumption $\Delta T =$ constant is therefore reasonable in a first approximation. The $A + \Delta T$-shared fit then enables us to separate the resonance effects (A_i) from the heating effect (ΔT). If this fit fails, then either $\Delta T =$ constant is wrong,

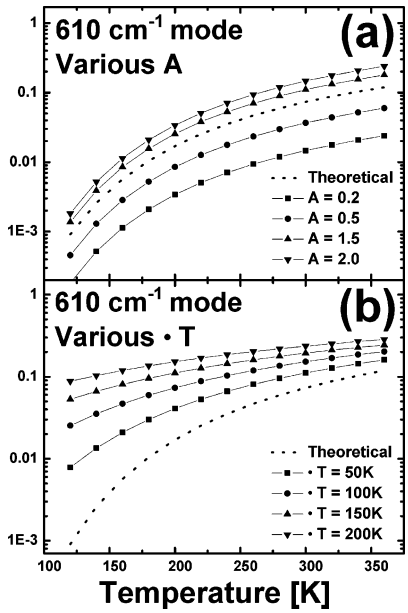

Figure 1. Theoretical plots showing the effect on the anti-Stokes/Stokes ratio of various values of A (a) and ΔT (b). Differing values of A result in nested anti-Stokes/Stokes ratios over the full temperature range. In the case of ΔT, the effect on the anti-Stokes/Stokes ratio varies across the full temperature range with the largest effect being made at lower temperatures, where ΔT represents a greater percentage of the initial temperature. This results in a "flaring out" of the ratio at lower temperatures which is noticeably larger for greater values of ΔT.

or the molecule is not in internal thermal equilibrium (i.e., pumping occurs). In the latter case, the effective mode temperature $T_0 + \Delta T_i$ is determined by the pumping rate, via eq 3. The fits with this model cannot therefore be valid, but the $A + \Delta T$ fit can still be useful in identifying which modes present an anomalous effective mode temperature and are therefore most likely to be pumped.

If the $A + \Delta T$-shared fit fails, the model above cannot distinguish directly between pumping (ΔT_i different for different modes) and temperature-dependent heating ($\Delta T_i = \Delta T$, but ΔT varies with T). To prove that different modes cannot be accounted for by a single T, we propose to define the following function (for two modes a and b):

$$F \equiv \frac{k_B \ln(\rho_a)}{\hbar\omega_a} - \frac{k_B \ln(\rho_b)}{\hbar\omega_b} \tag{6}$$

Then, describing each mode by an effective mode temperature, we have from eq 2

$$F \equiv C + \left[\frac{1}{T_a^{\text{eff}}} - \frac{1}{T_b^{\text{eff}}}\right] \tag{7}$$

where C is a constant accounting for the different A factors. The advantage of this function is as follows: if both modes share the same temperature, this function *is constant as a function of T*. The function F can be used to monitor relative changes between the effective T values of two modes as a function of external varying conditions (here T, but it could also be used to prove nonequilibrium pumping in a power-dependence experiment).

IV. Results and Discussion

A. Low Power. Example spectra for the 610 cm^{-1} RH6G mode under various experimental conditions are shown in Figure

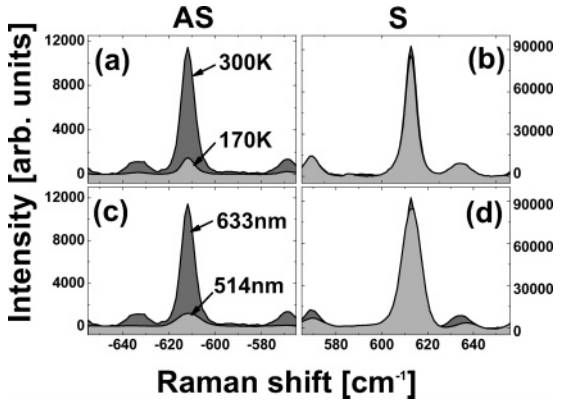

Figure 2. Example anti-Stokes (AS) (left) and Stokes (S) (right) spectra for the 610 cm^{-1} RH6G mode under various experimental conditions. Note the change in scale between the AS and S spectra. Panels a and b show the AS and S modes respectively at 300 (dark gray) and 170 K (light gray) for low power 633 nm excitation. It is clear that while there is little effect on the intensity on the Stokes side there is a significant decrease in the intensity of the AS signal as the temperature is decreased, as is expected from a decrease in thermal population. Panels c and d show the AS and S modes respectively for 633 (dark gray) and 514 nm (light gray) low power excitation at room temperature. We see a significant relative decrease in the intensity of the AS for the 514 nm with respect to the 633 nm line caused by the resonance profile. See the text for further details.

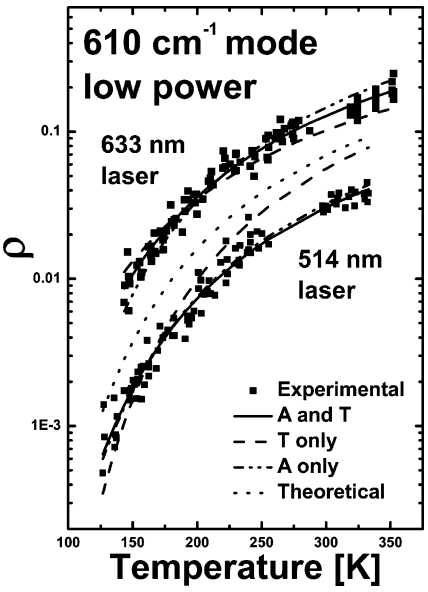

Figure 3. Anti-Stokes/Stokes ratios as a function of temperature for the 610 cm^{-1} SERS active modes of RH6G for the 633 and 514 nm lasers at low power (0.5 mW). There is a clear difference in the resonance contribution to the anomalous ratios between these lasers as the 633 nm ratio is increased above the theoretical value while the 514 nm ratio is suppressed below the theoretical value. The solid lines represent the fit to the experimental data with the $(A + \Delta T)$ model while the dashed and dash-dot lines represent the fits obtained from using only the ΔT or A parameter, respectively. The dotted line shows the theoretical ratio values. See the text for details.

2. Spectra a and b in Figure 2 show the AS and S modes respectively at 300 (dark gray) and 170 K (light gray) for low power 633 nm excitation. It is clear that while there is little effect on the intensity of the S modes, there is a significant decrease in the intensity of the AS modes as the temperature is decreased. This is expected from the decrease in the thermal population of the vibrational mode as the temperature is reduced and similar trends are observed for other modes. There is a corresponding decrease in the aS/S ratio as a function of temperature, which is described by eq 1. Spectra c and d in Figure 2 show the AS and S modes respectively for 633 (dark gray) and 514 nm (light gray) low power excitation at room temperature. There is a significant decrease in the intensity of the AS at 514 nm with respect to 633 nm while the intensity of the Stokes signal remains constant. This is consistent with both a resonance profile that peaks somewhere between 514 and 633 nm and previous results.[13]

Figure 3 shows examples of aS/S ratios as a function of T for the 610 cm^{-1} mode of RH6G and 633 nm excitation (top curve). The theoretically predicted behavior ($A = 1$, $\Delta T = 0$) and the fits to the experimental data with the $A + \Delta T$, A-only, and ΔT-only models are shown. The experimental data are well approximated by the $A + \Delta T$-shared fit for all modes investigated. The fitting to all the modes, using the four fitting procedures presented above, is summarized in Table 1. Figure 3 also shows the equivalent data for the 610 cm^{-1} mode under the 514 nm laser excitation (bottom curve). The AS peaks associated with the higher modes were too small to analyze at these laser powers. The $A + \Delta T$ fitting provides the best fit to the experimental data although ΔT is small and consequently the A-only model also fits the data reasonably well. The fitting results for the 610 cm^{-1} mode taken with the 514 nm laser are also summarized in Table 1.

The low power measurements tell us that the molecule is in thermal equilibrium with a heating of ~25 K when using the 633 nm laser and ~3 K when using the same low power 514 nm laser. This is despite the latter being closer to the bare molecular resonance and the single plasmon resonance of the individual colloids. However, this is consistent with our previous work[13] investigating resonance contributions to the anti-Stokes/Stokes ratio and it is attributed to a combined effect of collective plasmon resonances and the shift of the intrinsic resonance of the dye by the interaction with plasmons. A much larger coupling with the laser results at 633 nm than at 514 nm, accordingly.

Useful insight into the colloidal heating problem can be gained from considering a simplified 1-D model. Consider a single colloid where the laser power is assumed to dissipate through the top surface with no lateral heat flow. The T dependence of the thermal conductivity of Ag is small down to 40 K and we can use the room temperature value. The internal thermal time constant of the colloid (the time for the colloid to come to a uniform temperature), τ_c, is given by $\tau_c = C_{Ag}/K_c \approx 1 \times 10^{-11}$ s, where K_c is the thermal conductance of a single Ag particle (of size $\sim 20 \times 10^{-9}$ m^3) and C_{Ag} is the phononic contribution to the specific heat with Debye temperature, Θ_{Ag}, given by $C_{Ag} = c_{Ag}((D_{Ag}/MW_{Ag} \times 10^{-3}) \times d^3) \approx 6.1 \times 10^{-17}$ J/K. In this latter expression W_{Ag} is the atomic weight of Ag, D_{Ag} its density, d the length of the colloid, and $c_{Ag} \approx 7.8 \times 10^1$ J/(mol·K). We ignore the electronic contribution to c_{Ag} as it is much smaller than the phonon contribution, except at liquid He temperatures.

Assuming an incident power of 1 mW is focused into a 1 μm^2 area with a reflectivity of 80%, the number of photons absorbed per second by the colloid is $\approx 2.6 \times 10^{11}$ s^{-1}. Note that when dealing with small objects, τ_c is comparable to the arrival rate of the photons. The dynamics of the system is therefore rather interesting. The absorption of a single photon increases the colloid's upper surface temperature by $\approx 5.2 \times 10^{-3}$ K. By modeling the acoustic mismatch between Ag and Si,[19] we can estimate the expected increase in T. Estimating values from experimental data for interfaces between Al−Al_2O_3 and Pb−diamond, we find temperature increases of 2 and 10 K, respectively, which are of the right order of magnitude for

TABLE 1: Fitting Results for the 514 and 633 nm Lasers with Use of the Models Described in the Text[a]

	$A + \Delta T$-shared	$A + \Delta T$		A-only	ΔT-only
mode (cm^{-1})	A	A	ΔT (K)	A	ΔT (K)
		low power 633 nm laser			
610	1.30 ± 0.05 ($\Delta T = 25$ K)	1.50 ± 0.05	17 ± 5	2.00 ± 0.20	40 ± 5
780	1.35 ± 0.05 ($\Delta T = 25$ K)	1.65 ± 0.10	16 ± 5	2.35 ± 0.20	35 ± 5
1310	0.85 ± 0.10 ($\Delta T = 25$ K)	0.50 ± 0.10	55 ± 10	1.60 ± 0.30	20 ± 5
1360	0.95 ± 0.10 ($\Delta T = 25$ K)	0.80 ± 0.10	35 ± 5	1.90 ± 0.30	25 ± 5
1510	1.05 ± 0.10 ($\Delta T = 25$ K)	0.70 ± 0.10	40 ± 6	2.20 ± 0.40	30 ± 10
		high power 633 nm laser			
610	0.45 ± 0.05 ($\Delta T = 96$ K)	1.05 ± 0.10	40 ± 5	3.1 ± 0.5	40 ± 5
780	0.40 ± 0.04 ($\Delta T = 96$ K)	0.70 ± 0.10	60 ± 15	4.4 ± 1	50 ± 5
1310	0.50 ± 0.10 ($\Delta T = 96$ K)	0.15 ± 0.05	160 ± 35	12 ± 3	75 ± 10
1360	0.40 ± 0.10 ($\Delta T = 96$ K)	0.25 ± 0.10	120 ± 35	14 ± 3	70 ± 10
1510	0.50 ± 0.10 ($\Delta T = 96$ K)	0.08 ± 0.03	200 ± 40	20 ± 6	80 ± 10
		low power 514 nm laser			
610		0.45 ± 0.05	3 ± 2	0.50 ± 0.03	-20 ± 4

[a] Results are shown for both high and low power measurements for the 633 nm laser while only low power measurements were possible with the 514 nm laser. Low power means ~0.5 mW at the focal point while the high power measurement was an order of magnitude larger. All measurements were made on large colloidal clusters.The $A + \Delta T$ shared fitting is not possible for the 514 nm laser as only one mode was measurable. The $A + \Delta T$ shared and $A + \Delta T$ models provide the best representation of the data at low and high power respectively.

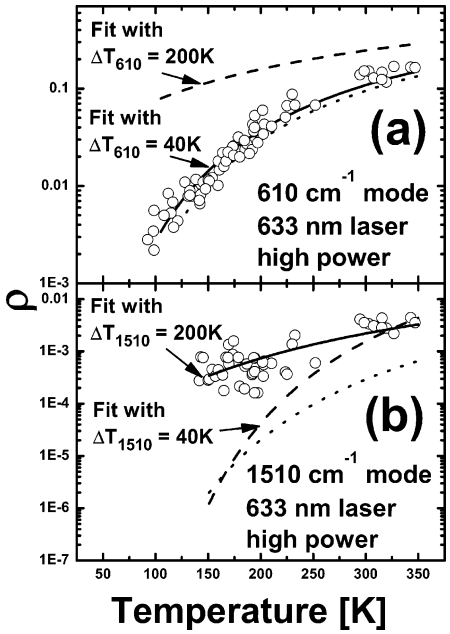

Figure 4. Anti-Stokes/Stokes ratio as a function of temperature for the 610 and 1510 cm^{-1} SERS active modes of RH6G taken with the 633 nm laser at high power (5 mW). The theoretically calculated ratio is shown as the dotted line. Two fits with the same value of A are shown for each mode. $\Delta T_{610} = 40$ K and $\Delta T_{1510} = 200$ K (solid lines) represents the best fit values for these modes. The secondary fits set $\Delta T_{610} = 200$ K and $\Delta T_{1510} = 40$ K (dashed lines).

our low power observations with the 633 nm laser. This is remarkable when we consider that we have ignored any potential contribution originating from SERS hot-spots and that the thermal model is extremely simplified. This model supports the scenario that at low powers the molecules could be heating through direct interaction with the colloids.

B. High Power. Figure 4 shows ρ as a function of T for the 610 and 1510 cm^{-1} modes for high power (5 mW) 633 nm excitation, while all other parameters were identical with the measurements at low power. We show the resulting fits of $A + \Delta T$ for both modes, as well as secondary fits swapping the temperatures and the theoretically expected ρ values. The high power ratios for all the modes were also fitted by using the $A + \Delta T$-shared model as in the low power data. This resulted in $\Delta T = 96$ K whereas the low power results gave 25 K. Although this is clearly larger, as would be expected, the quality of the fits was badly compromised for the high power data, as measured by a χ^2-test (not shown in the table). This indicates that this model is no longer valid in this regime. The results of the fitting to the high power 633 nm data for all the modes are also summarized in Table 1. Although photodecomposition of the analyte is reduced through the changing of the laser position for each measurement and averaging, it still affects the measurement. Under low power conditions, this effect was negligible but became more important for higher intensities and contributed to the greater scatter encountered under these conditions. This is included in the errors quoted.

The results in Table 1 show that the higher frequency modes have a lower A factor than lower modes for both the high and low power measurements. Some variation in the A factors between different modes is expected as a result of the changing contribution from the resonance profile over the spectral range of the measurement. This variation will depend on the specific shape of the resonance profile and the wavelength at which the measurement is made. There is a small variation in the values of A between the high and low power results attributed to an optically induced change in either the interaction of the analyte with the metal or the characteristic geometries of the clusters. The exact origin of this change is unknown at present and cannot be decided from these measurements by themselves.

The 610 cm^{-1} ratio as a function of T at high power is similar to that obtained at low powers; when plotted on the same graph it is almost impossible to separate them by eye suggesting that the mode temperature is not too dissimilar, despite an order of magnitude difference in the incident power. Indeed, the result of the $A + \Delta T$ fitting of the 610 cm^{-1} mode in both cases gives $\Delta T = 17 \pm 5$ K for low power and $\Delta T = 40 \pm 5$ K for high power, which is difficult to visualize on a log scale. For the 1510 cm^{-1} mode, although there is a great deal of scatter, there is a noticeable difference in the trend of the data when compared with the low power measurement. This behavior is very similar to the "flaring" of the theoretically determined ρ values for high ΔT as shown in Figure 1. This is confirmed with the fitting of the data to the A + ΔT model, which results in $\Delta T_{1510} = 200 \pm 40$ K, i.e., much larger than the $T_{610} = 40 \pm 5$ K from the best fit to the 610 cm^{-1} mode at high power. Figure 4 also shows fits for the 610 and 1510 cm^{-1} modes with $\Delta T_{610} = 200$ K and $\Delta T_{1510} = 40$, both with the best fit value of A for that

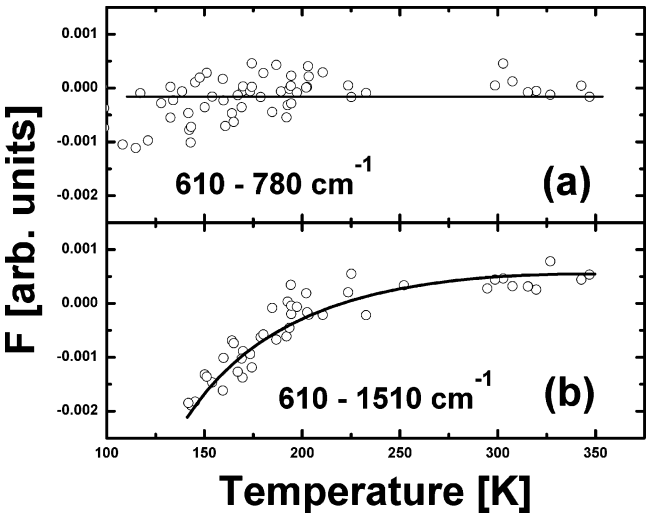

Figure 5. *F* function (eq 7) vs *T* comparing the effective temperatures of two different pairs of modes: (a) 780 and 610 cm^{-1} and (b) 1510 and 610 cm^{-1}. A constant value of *F* vs *T* in part a means that these two modes share a common temperature. The comparison in part b, however, points toward mode selective pumping of the 1510 cm^{-1} mode with respect to the 610 cm^{-1} mode. Solid lines are fits to the data. See the text for further details.

mode. It is obvious from these fits that the 610 cm^{-1} mode is much cooler than the 1510 cm^{-1} mode. All these results suggest that vibrational pumping in the 1510 cm^{-1} mode could be the explanation for the failure of the $A + \Delta T$-shared fits.

To explore this hypothesis, we plot in Figure 5 the function *F*, discussed in the previous section, which compares the effective *T* values of (Figure 5a) the 780 and 610 cm^{-1} modes and (Figure 5b) the 1510 and 610 cm^{-1} modes. The monotonic departure from a constant observed in Figure 5b is an additional demonstration of nonthermal equilibrium between these two modes and therefore in the molecule. This confirms that the failure of the $A + \Delta T$-shared fits is a consequence of vibrational pumping, and not of a temperature-dependent heating (same ΔT for all modes, but varying with temperature). In fact, the data in Figure 5 not only show evidence for mode specific pumping but also highlight the limitations of the $A + \Delta T$ model. The kink in *F* as a function of *T* means that the 1510, 780, and 610 cm^{-1} modes share a single *T* above ~200 K, while below that the 1510 cm^{-1} shows some mode specific pumping. This is only taken into account approximately in the $A + \Delta T$ model, and an equation such as that given by eq 3 needs to be used to account for pumping properly. Fits with eq 3 and 6 are also shown in Figure 5 and are in good agreement with the data. Moreover, we extract from the fit for the 1510 cm^{-1} mode a value of $\sigma_S \tau_r I_L = 5 \times 10^{-5}$. We estimate $I_L \approx 10^{24}$ photons/cm^2 and typical values for τ_r are in the range 1−10 ps. This leads to σ_S in the range 5×10^{-16} to 5×10^{-15} cm^2, compatible with previous estimates of the SERS cross section. We must point out that explicit interpretation of the measurement depends on the model of SERS enhancement,[8,10] which is highly debated in the literature. Regardless of this issue, the study of the *T* dependence of the function *F* certainly provides additional evidence that the behavior of the 1510 cm^{-1} below 200 K is a manifestation of vibrational pumping in this mode. This effect is more prominent at low *T* and for higher energy modes because the equilibrium population of the excited vibrational state is then very small and the relative change in intensity is larger. Following this argument, further evidence for pumping could be obtained from measurements at even lower temperatures ($T < 100$ K) than the ones accessed here. It also indicates that the modes are not strongly coupled to each other and are thus unable to thermalize quickly as described in the 4th scenario of section II. We note that the original paper on SERS pumping also presented some evidence for mode dependent effects.[8] Our results certainly contribute to this body of work and suggest that several mechanisms (vibrational pumping, underlying resonances, and colloid or SERS substrate heating) operate simultaneously and contribute together to the aS/S ratio anomalies.

In summary, we detail the key results presented in Table 1 as follows: (i) The $A + \Delta T$-shared model provides a satisfying agreement at low powers. The molecule is then in thermal equilibrium with a heating of ~25 K with respect to the substrate for the 633 nm laser, but only a ~3 K rise for 514 nm excitation which is be attributed to the molecular resonance being shifted by interaction with the metal surface. (ii) Models with only A or ΔT alone as fitting parameters systematically produce worse overall agreement with the data or even unphysical values, like negative heating (see for example the 610 cm^{-1} mode at 514 nm excitation in Table 1). (iii) For high powers using the 633 nm laser, an overall shared ΔT among the modes is not possible and one is forced to a better quality fit by allowing different effective temperatures for different modes. Using the function *F*, one can then demonstrate that this is the result of vibrational pumping in the 1510 cm^{-1} mode.

V. Conclusion

In closing, we have observed a laser frequency dependent heating of the order of 25 K at low laser power under SERS conditions with 633 nm excitation. We have shown that it is possible to decouple in dry samples the contributions of the thermal population and resonances in the aS/S ratios by performing a *T*-scan, thus overcoming the basic uncertainty in the different relative contributions which exist in studies at a single *T*. Most importantly, we have used this technique to provide evidence for at least two possible scenarios: a molecule in thermal equilibrium at low powers and mode specific pumping at high powers. Experiments at lower temperatures are in progress and will be reported elsewhere.

Acknowledgment. P.G.E. and L.F.C. acknowledge support by EPSRC (UK) under grant GR/T06124. R.C.M. acknowledges partial support from the National Physical Laboratory (UK) and the hospitality of the MacDiarmid Institute at Victoria University of Wellington, New Zealand.

References and Notes

(1) Moskovits, M. *Rev. Mod. Phys.* **1985**, *57*, 783.
(2) Otto, A. In *Light Scattering in Solids*; Cardona, M, Güntherodt, G., Eds.; Springer: Berlin, Germany, 1984; p 289.
(3) Faulds, K.; Barbagallo, R. P.; Keer, J. T.; Smith, W. E.; Graham, D. *Analyst* **2004**, *129*, 567.
(4) Green, M.; Lui, F. M.; Cohen, L. F.; Kollensperger, P.; Cass, A. *Faraday Discuss.* **2006**, *132*, in press.
(5) Storhofff, J. J.; Elghanian, R.; Mirkin, C. A.; Letsinger, R. L. *Langmuir* **2002**, *18*, 6666.
(6) Kneipp, J.; Kneipp, H.; Rice, W. L.; Kneipp, K. *Anal. Chem.* **2005**, *77*, 2381.
(7) Loo, C.; Lowery, A.; Halas, N.; West, J.; Drezek, R. *Nano Lett.* **2005**, *5*, 709.
(8) Kneipp, K.; Wang, Y.; Kneipp, H.; Itzkan, I.; Dasari, R. R.; Feld, M. S. *Phys. Rev. Lett.* **1996**, *76*, 2444.
(9) Maher, R. C.; Cohen, L. F.; Etchegoin, P.; Hartigan, H. J. N.; Brown, R. J. C.; Milton, M. J. T. *J. Chem. Phys.* **2004**, *120*, 11746.
(10) Haslett, T. L.; Tay, L.; Moskovits, M. *J. Chem. Phys.* **2000**, *113*, 1641.
(11) Brolo, A. G.; Sanderson, A. C.; Smith, A. P. *Phys. Rev. B* **2004**, *69*, 045424.

(12) Le Ru, E. C.; Etchegoin, P. G. *Faraday Discuss.* **2006**, *132*, in press.

(13) Maher, R. C.; Hou, J.; Cohen, L. F.; Liu, F. M.; Green, N.; Brown, R. J. C.; Milton, M. J. T.; Le Ru, E. C.; Hadfield, J. M.; Harvery, J. E.; Etchegoin, P. G. *J. Chem. Phys.* **2005**, *123*, 084702.

(14) Maher, R. C.; Cohen, L. F.; Le Ru, E. C.; Etchegoin, P. G. *Faraday Discuss.* **2006**, *132*, in press.

(15) Maher, R. C.; Dalley, M.; Le Ru, E. C.; Cohen, L. F.; Etchegoin, P. G.; Hartigan, H.; Brown, R. J. C.; Milton, M. J. T. *J. Chem. Phys.* **2004**, *121*, 8901.

(16) Kneipp, K.; Kneipp, H.; Itzkan, I.; Dasari, R. R.; Feld, M. S. *J. Phys.*: *Condens. Matter* **2002**, *14*, R597.

(17) Xu, H.; Aizpurua, J.; Käll, M.; Apell, P. *Phys. Rev. E* **2000**, 62, 4318.

(18) Lee, P. C.; Meisel, D. *J. Phys. Chem.* **1982**, 86, 3391.

(19) Cahill, D. G.; Ford, W. K.; Goodson, K. E.; Mahan, G. D.; Majumdar, A.; Maris, H. J.; Merlin, R.; Phillpot, S. R. *J. Appl. Phys.* **2003**, *93*, 793.